

AKÜ FEMÜBİD 20 (2020) 035901 (543-550)

AKU J. Sci. Eng. 20 (2020) 035901 (543-550)

DOI:10.35414/akufemubid.601054

Araştırma Makalesi / Research Article

Control of flow around Side by Side Square Prisms Using Control Rods

Mehmet SEYHAN^{1*}, Mustafa SARIOĞLU²^{1,2} Karadeniz Technical University, Engineering Faculty, Mechanical Engineering Department, Trabzon.

*Corresponding Author e-posta: mehmetseyhan@ktu.edu.tr ORCID ID: <https://orcid.org/0000-0002-5927-9128>
e-posta: sarioglu@ktu.edu.tr ORCID ID: <https://orcid.org/0000-0002-4295-7607>

Geliş Tarihi: 02.08.2019

Kabul Tarihi: 16.06.2020

Abstract

Keywords

Control rod; Square prism; Side by side; Drag coefficient

Flow characteristics around side by side square prisms with control rods are numerically investigated at different gap ratios (g^*) changing between 0.5 and 6 for $Re = 73$. Four different flow patterns, which are single street mode, irregular street mode, regular street mode and two street mode, are identified based on the gap ratio. Maximum drag reduction (%52) is obtained at $g^* = 6$. The mean lift coefficient has a symmetric variation between these gap ratios for the upper and lower square prisms. It can be concluded that the control rod is an effective flow control method in terms of drag reduction.

Kontrol Çubukları Kullanarak Yan Yana Kare Prizmalar Etrafındaki Akış Kontrolü

Öz

Anahtar kelimeler

Kontrol çubuğu; Kare prizma; Yan yana; Sürüklenme katsayısı

Kontrol çubuklu yan yana kare prizmalar etrafındaki akış karakteristikleri, $Re = 73$ için $g^* = 0.5 - 6$ aralığında değişen boşluk oranlarında nümerik olarak incelenmiştir. Tekli, ikili, düzensiz ve düzenli girdap caddesi olmak üzere dört farklı akış modeli boşluk oranlarına bağlı olarak tanımlanmıştır. Maksimum sürüklenme azalması (%52) $g^* = 6$ 'da elde edilmiştir. Ortalama kaldırma katsayısı, alt ve üst kare silindir için boşluk oranları arasında simetrik değişim göstermiştir. Kontrol çubuğunun sürüklenme kuvvetini azaltması açısından etkili bir akış kontrol yöntemi olduğu sonucu çıkarılabilir.

© Afyon Kocatepe Üniversitesi

1. Introduction

Due to vortex-induced vibration caused mechanical resonance, the collapse of three cooling tower at Ferrybridge power station (Khanduri *et al.* 1998) has drawn attention to solving this problem by many researchers including academic and engineering participant. Flow around the bluff and aerodynamic bodies is also encountered in many engineering application areas such as cooling towers, skyscrapers, bridges, heat exchangers, wind turbine towers, gas line pipe, and so on. As it is well known, flow control, therefore, occupy an important place to reduce or eliminate vortex-induced vibration (VIV), fluctuating drag force etc. on the flow around aerodynamics and blunt bodies such as a square prism and a circular cylinder. The flow control is classified as active (requiring energy spending) and

passive (not needing energy spending) flow control methods (Gad-el-Hak 1996). The active flow control (AFC) method include some processes such as dielectric barrier discharge (DBD) plasma actuator (Akbiyık *et al.* 2017, 2020), suction and blowing (Li *et al.* 2003, Müller *et al.* 2015), moving surface (Zhang *et al.* 2010) and so forth. Passive flow control (PFC) method consists of many different geometric modifications such as control rod (Sarioglu *et al.* 2005, Akansu *et al.* 2011, Fırat *et al.* 2015), splitter plate (Mansingh and Oosthuizen 1990, Sarioglu *et al.* 2006), trip wire (Bearman and Harvey 1993) etc. So far, these flow control methods for the single blunt body such as a circular cylinder and a square prism has been broadly studied in the literature. However, the alone bluff body is not commonly encountered. Therefore, bluff body configurations

such as side by side (Kang 2003, Inoue *et al.* 2006, Zhao 2013, Durga and Dhiman 2014, Mizushima and Hatsuda 2014), tandem (Sohankar and Etmianan 2009, Chatterjee and Amiroudine 2010) and staggered (Hu and Zhou 2008, Zhou *et al.* 2009) are used. Comprehensive available literature to the square prism in side by side arrangement and control rod will be summarized in the following paragraphs.

In PFC method including control rod, early studies on the flow around a square prism by using a rod was experimentally performed by Igarashi (1997). In this study, the effect of a control rod diameter (d) changing from 1 mm to 6 mm and a gap ratio between the rod and square prism was investigated at $Re = 3.2 \times 10^4$. His results showed that reduction in drag is %70 when it is compared with square prism alone. Akansu *et al.* (2011) researched the effect of attack angle changing between 0° and 90° on the flow around a square prism via control rod for $Re = 10000$. They showed that there is a significant drag reduction as well as heat transfer enhancement at 0° . In the study of Firat *et al.* (2015), the influence of control rod on the flow around the square prism is numerically investigated based on gap ratio and attack angle for $Re = 50-100$. They indicated that the seven different flow patterns observed depend on the attack angle. The total reduction in drag was %74 compared with square alone. In another geometric configuration, Yen and Liu (2011) experimentally researched the flow structure around the side by side square prisms at the range of $2262 < Re < 28000$ and $0 \leq g(\text{gap ratio}) \leq 12$. Their results indicated three different flow structures that are couple vortex-shedding mode, gap-flow mode, and single mode. While flow structure is the gap-flow mode, maximum drag reduction is obtained due to base bleeds between two square prisms. Alam and Zhou (2013) investigated the flow structure of a couple of square prisms in side by side via the dye flow visualization technic at $Re = 300$. They defined four flow phenomena, that are single bluff body, narrow and wide street regime, transition regime and the coupled-street regime, based on gap ratio. In the study of Prasad and Dhiman (2014), enhancement

of heat and momentum transfer around square prisms in side by side configuration is numerically investigated for steady and unsteady laminar flow at $10 \leq Re \leq 100$. Experimental parameters are chosen for Prandtl number changing from 0.5 to 50 and the gap ratio between square prisms varied from 1.5 to 10. Flow structure around tandem and side by side configuration for the square prisms was numerically implemented by Kondo *et al.* (1996). Their results indicated that flow structure for side by side and tandem configuration is a more complicated than that of the bare square prism.

As indicated above, studies were experimentally and numerically performed on the flow around a square prism with a control rod and a couple of square prisms for side by side configuration. But flow control around side by side square prisms with a control rod is not encountered in the literature. Therefore, the purpose of this study is to numerically elucidate the influence of the square prisms in side by side arrangement with two control rods and also fill this gap in the literature. The numerical study is performed for a constant center to center spacing ratio ($L/D = 1.5$), and different gap ratios between the square prisms ($G/D = 0.5, 1, 1.5, 2, 3, 4, 5$ and 6) and $Re = 73$.

2. Numerical Methods

Governing equation of the incompressible unsteady two-dimensional Navier-Stokes equations are considered. The governing equations can be written as follows:

$$\frac{\partial u_i}{\partial x_i} = 0 \quad (1)$$

$$\frac{\partial u_i}{\partial t} + u_j \frac{\partial u_i}{\partial x_j} = -\frac{1}{\rho} \frac{\partial p}{\partial x_i} + \nu \frac{\partial^2 u_i}{\partial x_i \partial x_j} \quad (2)$$

here u_i , and u_j are, respectively, velocity vector at x and y directions in cartesian coordinates, ν is the kinematic viscosity of the air, ρ is the density of the air and p is the pressure. Velocity and viscosity values are 0.05 and 2.74×10^{-2} , respectively, for the CFD computation.

In the present study, FLUENT[®] is used to solve the 2D unsteady incompressible laminar flow. Reynolds number based on length of the square prism is

chosen as 73. In terms of comparability with the literature, this Reynolds number has been chosen due to the study of Burattini and Agrawal (2013) investigating the side by side square cylinders at $Re=73$.

Pressure- velocity coupling is adopted as a semi-implicit pressure linked equation (SIMPLE). The time step is chosen as 0.01 s. Residuals for continuity, x and y velocity is smaller than 10^{-5} to stop the iteration.

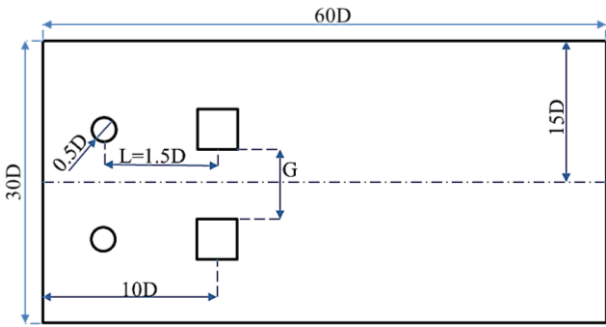


Figure 1. Schematic view of the computational domain.

The computational domain, choosing $30D \times 60D$ is illustrated in Fig. 1. The Twin squares are positioned $10D$ downstream and $50D$ upstream from the entrance. The models are centered $15D$ from lateral walls. In this numerical study, g^* (gap ratio) = $G/D = 0.5, 1, 1.5, 2, 3, 4, 5$ and 6 , and $Re = 73$ are considered as numerical parameter. The diameter ratio of the control rod (d) and the square prism (D) is $d/D = 0.25$. The gap between the control rod and the square prism is chosen as $L = 1.5D$.

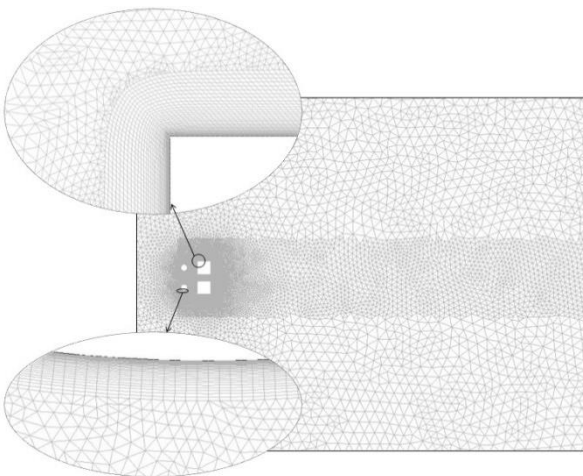


Figure 2. Detail view of the mesh structures around the model.

Boundary conditions for velocity inlet ($u=U_{\infty}, v=0$) and pressure outlet are set to the air inlet and

outlet, respectively. As shown in Fig. 1, the no-slip boundary condition is applied to showing as a bold line including rods, squares and side walls ($u=0$ and $v=0$). Pressure outlet condition is applied as “0”. Unstructured mesh strategy is adopted for this model because of easy applicability for every geometrical model. Triangular mesh structure generated is shown in Fig. 2. Boundary layer mesh adaption is used for mesh structure around the square prisms and control rods. The first layer thickness of mesh near the wall of its is set as $0.0001D$. Mesh independence test is performed by using a mesh adaption feature of FLUENT.

Initially, the coarse generated mesh is computed up to flow fully developed and after two times, the mesh adaption is applied. Discrepancies for Strouhal number, lift coefficient and drag coefficient are about $\%7.2, \%2.7$ and $\%0.5$ with final mesh adaption. As shown in Table 1, these results show that the mesh size is sufficient to investigate the flow structure on the flow control around the side by side square prisms without the control rods. As given in table 1, the study of Burattini and Agrawal (2013), investigating control of flow around the side by side square prisms for $g^*=0.5$ at $Re=73$ are used in order to verify this simulation.

Table 1. Mesh independence test and numerical method validation for side by side square prisms without the control rod for $g^*=0.5$ at $Re=73$.

	Mesh	C_{d2s}	C_{d1s}	C_{l2s}	C_{l1s}	St
Present study	127564	2.13	2.03	0.941	-1.055	0.082
Present study	453112	1.97	2.05	0.919	-1.009	0.085
Present study	580420	1.95	2.02	0.921	-0.997	0.097
Burattini and Agrawal (2013)	-	-	2.01	-	-0.97	0.095

3. Numerical Results and Discussion

In this study, the influence of the control rods on the flow control around side by side square prisms is numerically investigated in terms of mean drag and lift coefficient, and the vortex shedding pattern. Figure 3(a) shows changes in the mean lift coefficient versus gap ratio varied from 0.5 to 6 for the square prism. The mean lift coefficient has a

symmetric variation between these gap ratios for the upper ($C_{L_{2s}}$) and the lower ($C_{L_{1s}}$) squares. In other words, if the sign of $C_{L_{1s}}$ inverts, these values show the same trend with $C_{L_{2s}}$. When increased the gap ratio, C_L for each model decreases to a value close to 0. While gap ratio has the smallest value, up and downside the square periodically push each other

because of increasing the pressure differences between the upper and lower side of its so the mean absolute lift coefficients for squares obtain as 0.9. The lower square lift coefficient variation shows nearly the same trend with the study of Burattini and Agrawal (2013) that is side by side square prism configuration without a rod.

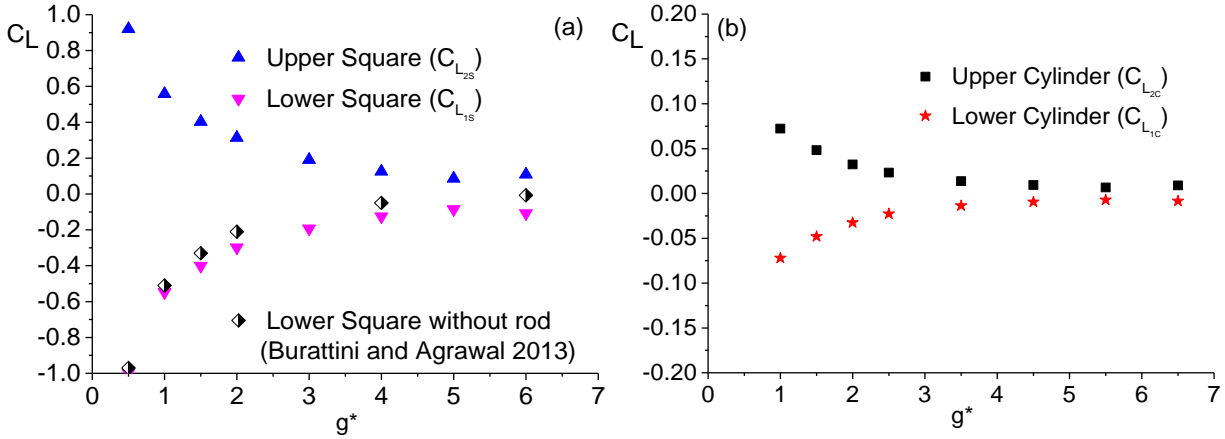


Figure 3. Mean lift coefficient versus gap ratio for (a) square prisms and (b) control rod.

Figure 3(b) indicates the averaged lift coefficient versus gap ratio changing between 1 and 6.5 for the control rod having a circular geometry. As it was in square lift coefficient variation based on g^* , it has a symmetric variation between these gap ratios for the upper ($C_{L_{2c}}$) and the lower ($C_{L_{1c}}$) circular prisms. The mean absolute lift coefficient ($\langle C_L \rangle$) has the highest value that is 0.072 for $g^* = 1$. While increasing g^* , $\langle C_L \rangle$ is almost close to 0.

Effects of variation of the gap ratios on the mean drag coefficient and drag reduction (DR) are presented in Figure 4. When looking at this plot, on the one hand C_d of square prisms significantly decreases by increasing gap ratio, but on the other hand C_d of circular prisms slightly increases. The mean drag coefficient of the upper ($C_{d_{2s}}$) and the lower ($C_{d_{1s}}$) squares has nearly the same values for all gap ratio. The change in C_d for the study of Burattini and Agrawal (2013) is represented by green symbols and also DR is calculated using present and Burattini and Agrawal (2013) study. Minimum drag reduction is obtained as %30 for $g^* = 0.5$. While g^* increase from 0.5 to 6, drag reduction indicates an increasing trend and also reaches the maximum value (%52) at $g^* = 0.5$.

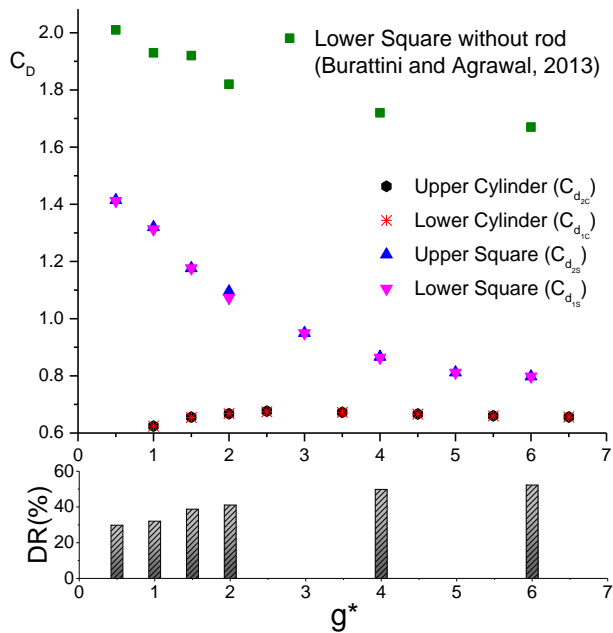


Figure 4. Mean drag coefficient versus gap ratio changing between 0.5 and 6 for $Re = 73$.

In the study of Inoue *et al.* (2006), they indicated that flip-flopping flow pattern is obtained for side by side square prisms at $g^* = 1.5$ and 2. Flip-flopping flow pattern expresses two asymmetric states in the wake region and symmetric instantaneous drag and lift coefficient distributions (Kang 2003, Inoue *et al.* 2006). At $g^* = 2$, Figure 5 (a and b) indicates the evolutions of the lift and drag coefficient, respectively. As stated by Kang (2003) and Inoue *et al.* (2006), Flip-flopping flow pattern is seen in these

figures. These results are also supported with vortex shedding flow pattern given in Figure 7.

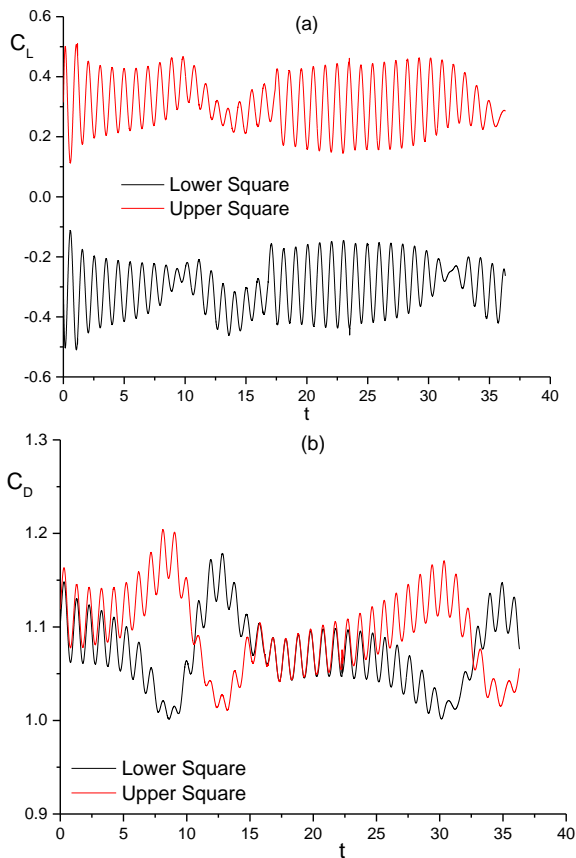


Figure 5. Time history of (a) lift coefficient and (b) drag coefficient for square prisms at $g^* = 2$

Effects of side by side square prisms with the control rods on the Strouhal number, expressed by $St = fD/u$, according to variation of gap ratio between square prisms are presented in Figure 6. In the range of $0.5 \leq g^* \leq 6$, the Strouhal number of square prisms with control rod is lower than that of square prisms without the control rod for the study of Burattini and Agrawal (2013). In addition, the variations of the St for the present study show similar trend with the study of Burattini and Agrawal (2013). At $g^* = 0.5$, reduction in the St number for square prism with the control rod is 20.8% as compared to square prism without the control rod. The St number for the square prism without the control rod are in good agreement with the results of Burattini and Agrawal (2013). The Strouhal number quickly increases with increasing g^* between 0.5 and 1.5. The St number is nearly constant at a value around 0.15 in the range of $1.5 \leq g^* \leq 6$. Therefore, the distribution of Strouhal number is nearly independent from gap

ratio (g^*) between 1.5 and 6. The variation of the Strouhal number in these gap ratios is qualitatively almost similar to that obtained by Bearman and Wadcock (1973) and Burattini and Agrawal (2013). As a result, it was seen that the control rod generally reduces the Strouhal number.

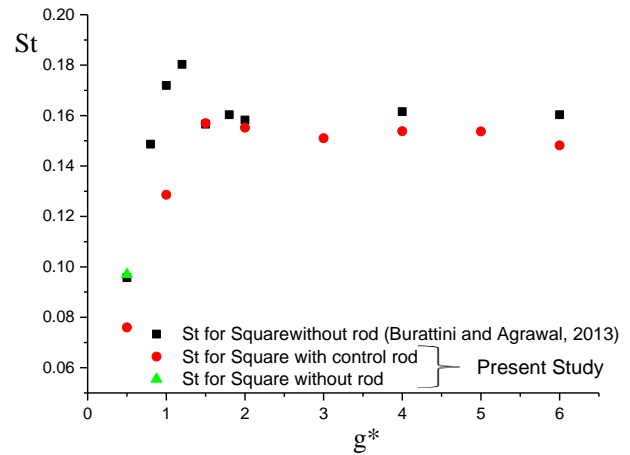


Figure 6. Variation of the Strouhal number with g^* changing between 0.5 and 6 for $Re = 73$.

Figure 7 indicates the vortex shedding patterns on the flow control around side by side square prism with the control rod for $g^* = 0.5, 1, 1.5, 2, 3, 4, 5$ and 6. The vortex shedding around the model forms a single row vortex street for with/without rod at $g^* = 0.5$. But side by side squares with control rods significantly delay the vortex shedding and they have been clearly seen in Figure 6. This flow pattern is called a single street mode. Some vortices move across the centerline with close interaction with the other vortices at $g^* = 1$. While g^* is 2, vortices behind the side by side prisms with control rod merge into the other vortices in the downstream wake. At $1 \leq g^* \leq 2$, there are irregular vortex street and this irregularity of vortex street increases while being increased the g^* . The flow pattern is named as an irregular street mode. After this gap ratio, regular and symmetric vortex streets in accordance with the centerline appear up to $g^* = 6$. While g^* is between 3 and 5, the obtained flow pattern is called as regular vortex street mode. At $g^* = 6$, there is two vortex streets behind the model, and also vortex shedding slightly shifts and loses the symmetry flow pattern that is named as two street mode.

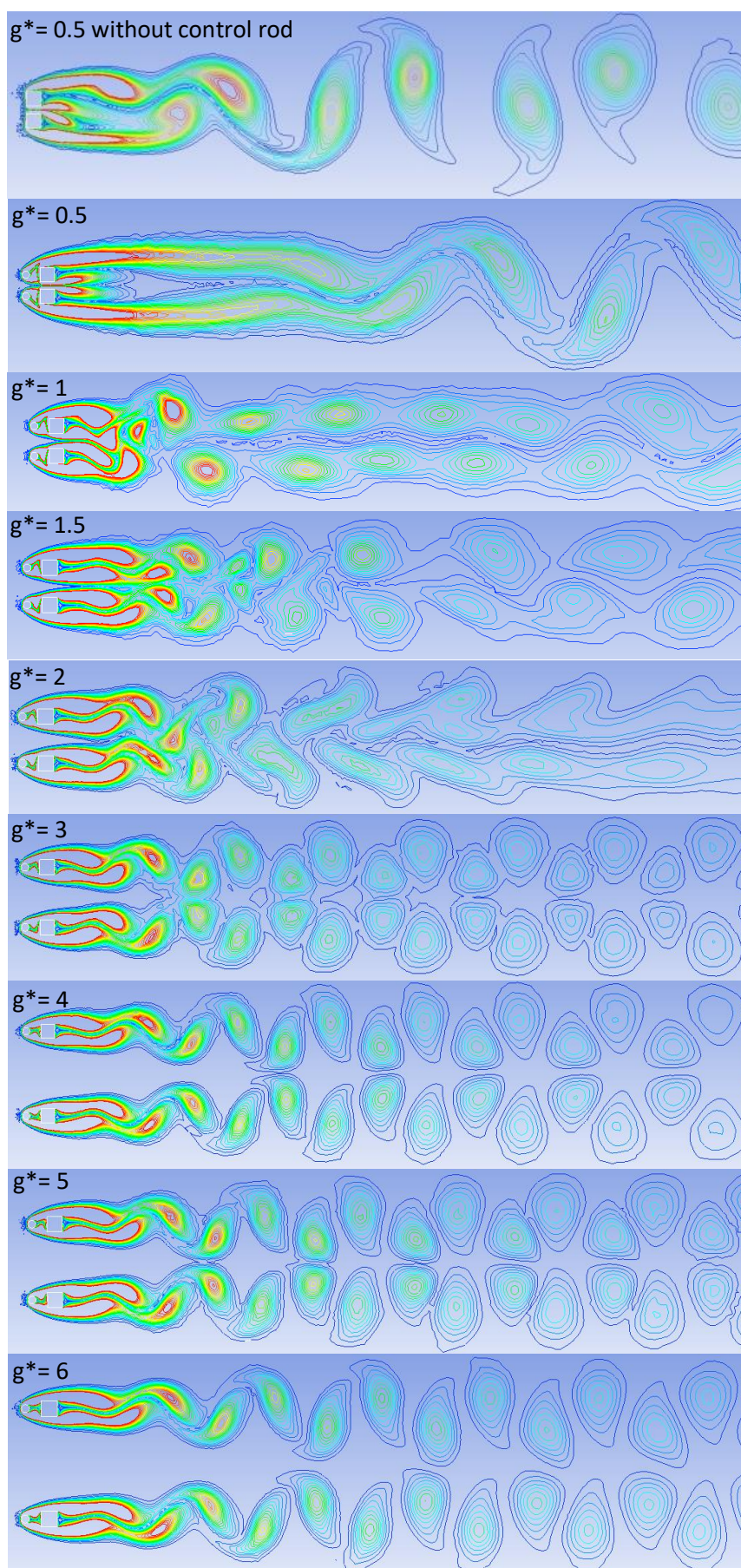


Figure 7. Vortex shedding pattern on the flow control around side by side square prism with control rod for $g^* = 0.5, 1, 1.5, 2, 3, 4, 5$ and 63

4. Conclusion

The flow control around the side by side square prisms with rods is conducted to investigate the flow characteristics such as vortex street patterns, drag and lift coefficients at $Re = 73$ and $g^* = 0.5, 1, 1.5, 2, 3, 4, 5$ and 6 . The remarkable findings for the side by side square prisms with the rods can be summarized as follows;

1. For the square prisms with rods compared with the square prism alone, maximum and minimum drag reduction (%52 and 30) is obtained at $g^* = 6$ and 0.5 , respectively. It could be inferred that the use of the control rod is an effective flow control method in terms of drag reduction.
2. Based on the gap ratio, four different flow patterns are described. These are single street mode, irregular street mode, regular street mode and two street mode.
3. It could be also inferred that the control rod is no significant effect on the mean lift coefficient acting on the square prism.
4. The Strouhal number is independent of g^* in the range of $1.5 \leq g^* \leq 6$

5. References

- Akansu, Y.E., Ozmert, M. and Firat, E., 2011. The effect of attack angle to vortex shedding phenomenon of flow around a square prism with a flow control rod. *Isi Bilimi Ve Teknigi Dergisi-Journal Of Thermal Science And Technology*, **31** (1), 109–120.
- Akbıyık, H., Akansu, Y.E. and Yavuz, H., 2017. Active control of flow around a circular cylinder by using intermittent DBD plasma actuators. *Flow Measurement and Instrumentation*, **53**, 215–220.
- Akbıyık, H., Yavuz, H. and Akansu, Y.E., 2020. Aerodynamic and energy-efficiency-based assessment of plasma actuator's position on a NACA0015 airfoil. *Contributions to Plasma Physics*, **60** (2), e201900009.
- Alam, M.M. and Zhou, Y., 2013. Intrinsic features of flow around two side-by-side square cylinders. *Physics of Fluids*, **25** (8), 085106.
- Bearman, P.W. and Harvey, J.K., 1993. Control of circular cylinder flow by the use of dimples. *AIAA journal*, **31** (10), 1753–1756.
- Bearman, P.W. and Wadcock, a. J., 1973. The interaction between a pair of circular cylinders normal to a stream. *Journal of Fluid Mechanics*, **61** (03), 499.
- Burattini, P. and Agrawal, A., 2013. Wake interaction between two side-by-side square cylinders in channel flow. *Computers & Fluids*, **77**, 134–142.
- Chatterjee, D. and Amiroudine, S., 2010. Two-dimensional mixed convection heat transfer from confined tandem square cylinders in cross-flow at low Reynolds numbers. *International Communications in Heat and Mass Transfer*, **37** (1), 7–16.
- Durga Prasad, A.V.V.S. and Dhiman, A.K., 2014. CFD Analysis of Momentum and Heat Transfer Around a Pair of Square Cylinders in Side-by-Side Arrangement. *Heat Transfer Engineering*, **35** (4), 398–411.
- Firat, E., Akansu, Y.E. and Akilli, H., 2015. Flow past a square prism with an upstream control rod at incidence to uniform stream. *Ocean Engineering*, **108**, 504–518.
- Gad-el-Hak, M., 1996. Modern developments in flow control. *Applied Mechanics Reviews*, **49** (7), 365–379.
- Hu, J.C. and Zhou, Y., 2008. Flow structure behind two staggered circular cylinders. Part 1. Downstream evolution and classification. *Journal of Fluid Mechanics*, **607**, 51–80.
- Igarashi, T., 1997. Drag reduction of a square prism by flow control using a small rod. *Journal of Wind Engineering and Industrial Aerodynamics*, **69**, 141–153.
- Inoue, O., Iwakami, W. and Hatakeyama, N., 2006. Aeolian tones radiated from flow past two square cylinders in a side-by-side arrangement. *Physics of Fluids*, **18** (4), 046104.
- Kang, S., 2003. Characteristics of flow over two circular cylinders in a side-by-side arrangement at low Reynolds numbers. *Physics of Fluids*, **15** (9), 2486–2498.
- Khanduri, A.C., Stathopoulos, T. and Bédard, C., 1998. Wind-induced interference effects on buildings — a review of the state-of-the-art. *Engineering Structures*, **20** (7), 617–630.
- Kondo, N., Nishimura, T. and Yamada, S., 1996. Third-order upwind finite element simulation of flow around two square cylinders. *International Journal of Computational Fluid Dynamics*, **7** (1–2), 143–153.
- Li, Z., Navon, I.M., Hussaini, M.Y. and Le Dimet, F.X., 2003. Optimal control of cylinder wakes via suction and blowing. *Computers and Fluids*, **32** (2), 149–171.
- Mansingh, V. and Oosthuizen, P.H., 1990. Effects of splitter plates on the wake flow behind a bluff body.

AIAA journal, **28** (5), 778–783.

Mizushima, J. and Hatsuda, G., 2014. Nonlinear interactions between the two wakes behind a pair of square cylinders. *J. Fluid Mech.*, **759**, 295–320.

Müller-Vahl, H.F., Strangfeld, C., Nayeri, C.N., Paschereit, C.O. and Greenblatt, D., 2015. Control of Thick Airfoil, Deep Dynamic Stall Using Steady Blowing. *AIAA Journal*, **53** (2), 277–295.

Sarioğlu, M., Akansu, Y.E. and Yavuz, T., 2005. Control of the flow around square cylinders at incidence by using a rod. *AIAA journal*, **43** (7), 1419–1426.

Sarioğlu, M., Akansu, Y.E. and Yavuz, T., 2006. Flow around a rotatable square cylinder-plate body. *AIAA journal*, **44** (5), 1065–1072.

Sohankar, A. and Etminan, A., 2009. Forced-convection heat transfer from tandem square cylinders in cross flow at low Reynolds numbers. *International Journal for Numerical Methods in Fluids*, **60** (7), 733–751.

Yen, S.C. and Liu, J.H., 2011. Wake flow behind two side-by-side square cylinders. *International Journal of Heat and Fluid Flow*, **32** (1), 41–51.

Zhang, Y.Y., Huang, D.G., Sun, X.J. and Wu, G.Q., 2010. Exploration in optimal design of an airfoil with a leading edge rotating cylinder. *Journal of Thermal Science*, **19** (4), 318–325.

Zhao, M., 2013. Flow induced vibration of two rigidly coupled circular cylinders in tandem and side-by-side arrangements at a low reynolds number of 150. *Physics of Fluids*, **25** (12), 123601.

Zhou, Y., Feng, S.X., Alam, M.M. and Bai, H.L., 2009. Reynolds number effect on the wake of two staggered cylinders. *Physics of Fluids*, **21** (12), 125105.